

BARYCENTER KINEMATICS IN LOCAL GROUP ANALOGUES

I. A. LÓPEZ-PAREDES 

Tecnológico de Monterrey, Escuela de Ingeniería y Ciencias, Ave. Eugenio Garza Sada 2501, Monterrey 64849, NL, Mexico

J. E. FORERO-ROMERO 

Departamento de Física, Universidad de los Andes, Cra. 1 No. 18A-10 Edificio Ip CP 111711 Bogotá, Colombia;
je.forero@uniandes.edu.co and
Observatorio Astronómico, Universidad de los Andes, Cra. 1 No. 18A-10 Edificio H CP 111711 Bogotá, Colombia

Version June 12, 2025

ABSTRACT

We present a new way to identify systems similar to our Local Group (LG) of galaxies in cosmological simulations. Our method uses as a new constraint the speed and direction of the LG’s center of mass, which we can measure accurately from cosmic microwave background data. When we apply these criteria to different cosmological simulations and compare the results with traditional selection methods, we find statistically significant differences. Our approach produces simulated galaxy pairs where the relative M31 velocity is less radial (2% to 10% difference over the mean) and more tangential (1% to 4% difference over the mean) than in cases that do not take into account the barycenter speed. The radial change pattern appears consistently across all cosmological models we test, showing that matching the observed barycenter velocity has a measurable effect when modeling and interpreting Local Group-like systems.

Subject headings: Local Group, N-body simulations, barycenter kinematics

1. INTRODUCTION

Understanding the orbit between M31 and the Milky Way (MW) is key to explaining how the Local Group (LG) evolved (Hartl & Strigari 2024). Recent research challenges the old view that this orbit is mostly head-on (radial), suggesting instead that it has more sideways motion than previously thought (van der Marel et al. 2019; Salomon et al. 2021). These studies rely on cosmological simulations to establish expectations for the tangential velocity components. To study LG dynamics, previous work typically identify similar galaxy pairs in simulations by applying specific criteria to halo pairs, including their masses, approach speed, distance, and isolation from other large structures (Forero-Romero et al. 2013; Sawala et al. 2023; Hartl & Strigari 2022).

We identified an important measurement that previous studies haven’t used when defining LG-like systems. This measurement is the LG’s barycenter velocity (\mathbf{v}_b), which we can determine precisely from cosmic microwave background (CMB) data (Planck Collaboration et al. 2020). We use this constraint in two ways. First, we consider its magnitude (v_b). Second, we examine the direction, measured as the angle (θ) between the barycenter velocity vector and the position vector from MW to M31 (\mathbf{r}), as shown in Figure 1. We express this angle more conveniently as $\mu = \cos \theta$, which comes from the dot product of the unit vectors for \mathbf{v}_b and \mathbf{r} .

Previous studies couldn’t use the barycenter velocity because they worked with simulations that were too small in volume. Recently, Forero-Romero & Sierra-Porta (2022) showed that peculiar velocities can be in-

accurate in small simulation boxes due to power spectrum limitations. Using simulations with volumes ranging from 100 to 2967 Mpc across, they demonstrated that accurate kinematic properties require boxes at least 1 Gpc across. Both theoretical arguments and simulation results support this conclusion.

In this paper, we use simulations to measure how including the barycenter velocity constraint affects the predicted radial and tangential velocities of M31 relative to the MW. We also explore how these effects vary across simulations with different cosmological parameters.

Our paper is organized as follows: Section 2 covers the observational constraints, Section 3 describes our simulations and the different cosmological models. In Section 4, we explain how we select LG analogues using both *traditional* criteria and our new approach. Section 5 presents and discusses our findings, and Section 6 summarizes our conclusions.

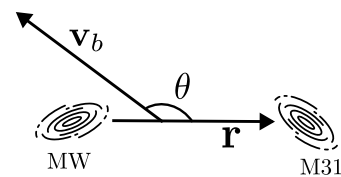


FIG. 1.— Diagram showing the alignment between key quantities used to select LG analogues. \mathbf{v}_b represents the barycenter velocity of the LG and \mathbf{r} shows the relative position from M31 to the MW

arXiv:2505.04054v2 [astro-ph.GA] 9 May 2025

TABLE 1

SUMMARY OF OBSERVED REFERENCE VALUES. THE COLUMNS REPRESENT, RESPECTIVELY: THE PHYSICAL OBSERVABLE, ITS MEASURED VALUE, THE CORRESPONDING UNITS, AND THE BIBLIOGRAPHIC SOURCE.

Observable	Value	Units	Source
v_b	620 ± 15	km s^{-1}	Planck Collaboration et al. (2020)
$(l, b)_{v_b}$	$(271.9 \pm 2.0, 29.6 \pm 1.4)$	deg	Planck Collaboration et al. (2020)
r_{MW}	8.29 ± 0.16	kpc	McMillan (2011)
$(l, b)_{\text{MW}}$	$(359.944215 \pm 0.000006, -0.046079 \pm 0.000009)$	deg.	Yusef-Zadeh et al. (1999)
r_{M31}	761 ± 11	kpc	Li et al. (2021)
$(l, b)_{\text{M31}}$	$(121.174409 \pm 0.000022, -21.572996 \pm 0.000022)$	deg.	Evans et al. (2010)
$v_{r, \text{M31}}$	-109.3 ± 4.4	kms^{-1}	van der Marel et al. (2012)
$v_{t, \text{M31}}$	82.4 ± 31.2	kms^{-1}	Salomon et al. (2021)
μ	-0.88 ± 0.01	adim.	This work

2. OBSERVATIONAL CONSTRAINTS

Table 1 summarizes the key observational values used to calculate μ . We obtain the barycenter velocity of the LG from cosmic microwave background (CMB) measurements (Planck Collaboration et al. 2020). The positions of both M31 and the MW are well known from previous studies. For the Sun-to-Galactic Center distance, we use the value from McMillan (2011), who derived this by fitting MW mass models to observational data. The Galactic Center position comes from VLA measurements reported by Yusef-Zadeh et al. (1999). For M31, we use the distance measured by Li et al. (2021) using Cepheid variable stars, and coordinates from the Chandra Source Catalog (Evans et al. 2010).

To calculate the relative position vector from M31 to MW (\mathbf{r}) and determine μ , we use a Monte Carlo approach. We build a covariance matrix using coordinate measurement error ellipses (from NASA/IPAC Extragalactic Database) and sample from a multivariate normal distribution. The uncertainties in Table 1 represent the standard deviations of these samples. Our method yields an M31-MW separation of 765 ± 11 kpc, matching observations reported by Chamberlain et al. (2022). To compute μ , we generate normal distribution samples for \mathbf{v}_b and the distances to MW and M31. We then compute the dot product between \mathbf{v}_b and \mathbf{r} , finding $\mu = -0.88 \pm 0.01$. This result shows a strong anti-alignment between these vectors.

3. SIMULATION

For this study, we use the AbacusSummit simulation suite (Maksimova et al. 2021; Garrison et al. 2021). We analyze the base simulation box with 6912^3 particles in a $2 \text{ Gpc}/h$ volume. Because the simulation snapshot is at redshift $z = 0.1$, we use the halos’ peculiar velocities to project their positions to present-day values.

We begin with the primary cosmology (c000), which uses the Planck2018 ΛCDM model with massive neutrinos. We then analyzed 91 additional cosmologies. These include: c009 (without neutrino mass), c019 and c020 (with varied neutrino species counts), and four secondary cosmologies (c001-c004) that test different scenarios such as low Ω_c , wCDM (c002), high N_{eff} , and low σ_8 .

We also study ten reference cosmologies (c010, c012-c018, c021-022) that match models from other major projects, mostly using massless neutrinos. For wider parameter testing, we include simulations with a linear derivative grid (c100-c116) with small changes across eight parameters, and an unstructured emulator grid (c130-c181) covering broader parameter ranges. All cos-

mologies use the same τ value (0.0544) and most included 60 meV neutrinos, consistent with Planck 2018 results.

4. SELECTION OF LG ANALOGUES

We use halos identified with the CompaSO Halo Finder (Hadzhiyska et al. 2021), with selection criteria similar to those in Forero-Romero & Sierra-Porta (2022). We selected halos with maximum circular velocities $V_{\text{max}} > 200 \text{ km s}^{-1}$.

From these, we identify isolated pairs as two halos, A and B, that are each other’s nearest neighbors. We also require that no third halo with a maximum circular velocity greater than halo B’s can be found within three times the pair’s separation distance. We define halo A as the one with the greater maximum circular velocity, which we designated as M31. This forms our main sample, typically containing about 8×10^5 pairs per simulation box.

From this main sample, we create two subsamples:

The first subsample, which we call *traditional*, includes pairs meeting these conditions:

- Total pair mass between $[0.5, 5.0] \times 10^{12} M_{\odot}$
- Separation between halos less than $1 \text{ Mpc } h^{-1}$
- Negative radial relative velocity of M31 with respect to the MW ($v_r < 0 \text{ km s}^{-1}$), after accounting for cosmic expansion

The second subsample, which we call *realistic*, includes all the *traditional* criteria plus these additional barycenter velocity conditions:

- Barycenter speed greater than the observed value ($v_b > 620 \text{ km s}^{-1}$)
- Alignment value less than the observed value ($\mu < -0.88$)

We use inequalities rather than narrow ranges around the observed values because this approach: (1) captures the observed trends that the barycenter speed is unusually high and the alignment shows strong anti-alignment, and (2) allows us to keep more pairs in our sample that satisfy these conditions.

The *traditional* subsample typically contains about 2×10^5 pairs per simulation box, while the *realistic* sample contains about 10^4 pairs.

4.1. Statistical Tests

Using the simulations, we compute the cumulative probability distributions for μ and three key Local Group properties:

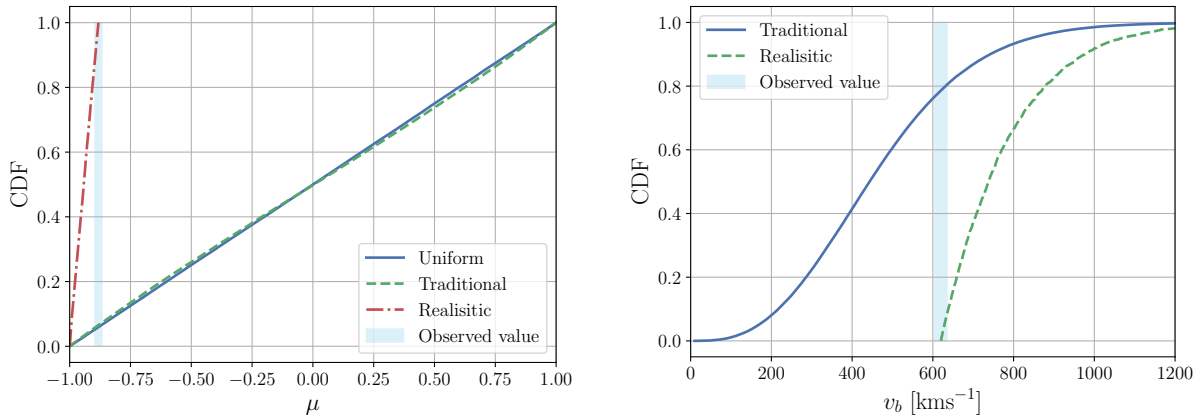


FIG. 2.— Left panel: cumulative distribution of μ , the cosine of the angle between the barycenter velocity of the LG and the relative position vector from M31 to the MW. Right panel: Cumulative distribution for the barycenter speed v_b of the Local Group.

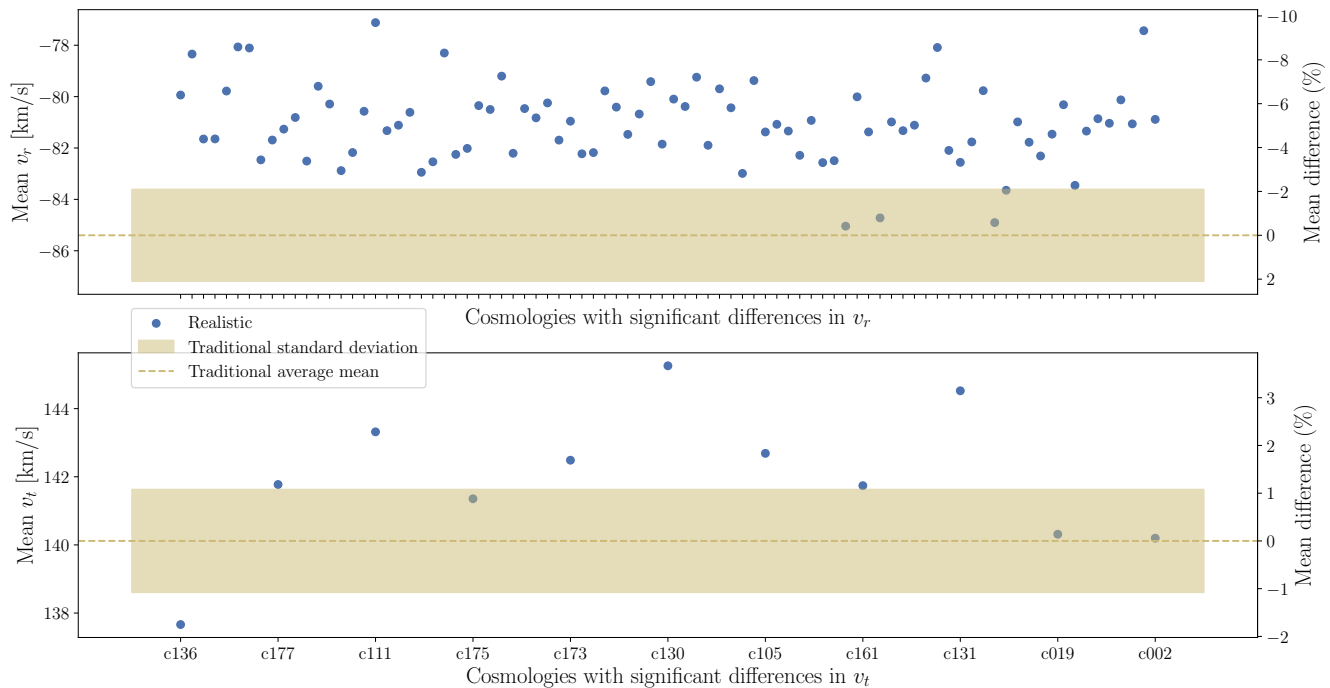


FIG. 3.— Impact of our proposed barycenter velocity constraints on the mean velocity distributions of M31. Only cosmologies with statistically significant differences are shown. Dashed lines and shaded regions represent the average and standard deviation of the mean values across *traditional* pair distributions for all cosmologies. The secondary y-axis shows the percentage difference in mean values compared to the average mean of *traditional* pairs.

- Total Local Group mass (M_{LG})
- Radial velocity of M31 relative to the MW (v_r)
- Tangential velocity of M31 relative to the MW (v_t)

To measure how our barycenter velocity constraints affect these properties, we compare the mean values between the *traditional* and *realistic* pair distributions. We also use two-sample Kolmogorov–Smirnov (KS) tests to determine if these differences are statistically significant, with p -values below 0.05 considered significant.

5. RESULTS

5.1. Base cosmology

Figure 2 shows the cumulative distributions of μ and v_b in the base cosmology (c000). These distributions illustrate the key features of our barycenter velocity constraints used to select LG analogues. The μ distribution reveals that \mathbf{v}_b and \mathbf{r} in simulated LG pairs tend to be either aligned or anti-aligned. We confirm this by comparing against a uniform distribution using a KS test, which shows statistically significant differences ($p < 0.05$). Using the same statistical method, we also find that the distribution is not symmetric with a slight tendency towards anti-alignment.

We find statistically significant differences between *traditional* and *realistic* pairs in M31’s radial velocity distribution. For radial velocity (v_r), the mean value increases

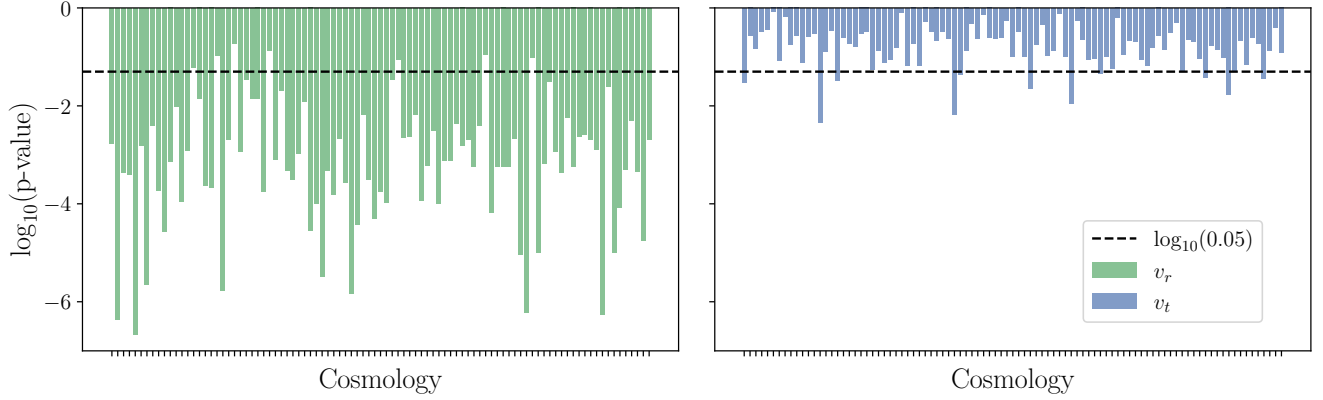


FIG. 4.— Statistical significance of the differences between *realistic* and *traditional* selection criteria for radial velocity v_r (left column) and tangential velocity v_t (right column). The p -values shown are from two-sample Kolmogorov-Smirnov tests across all cosmologies.

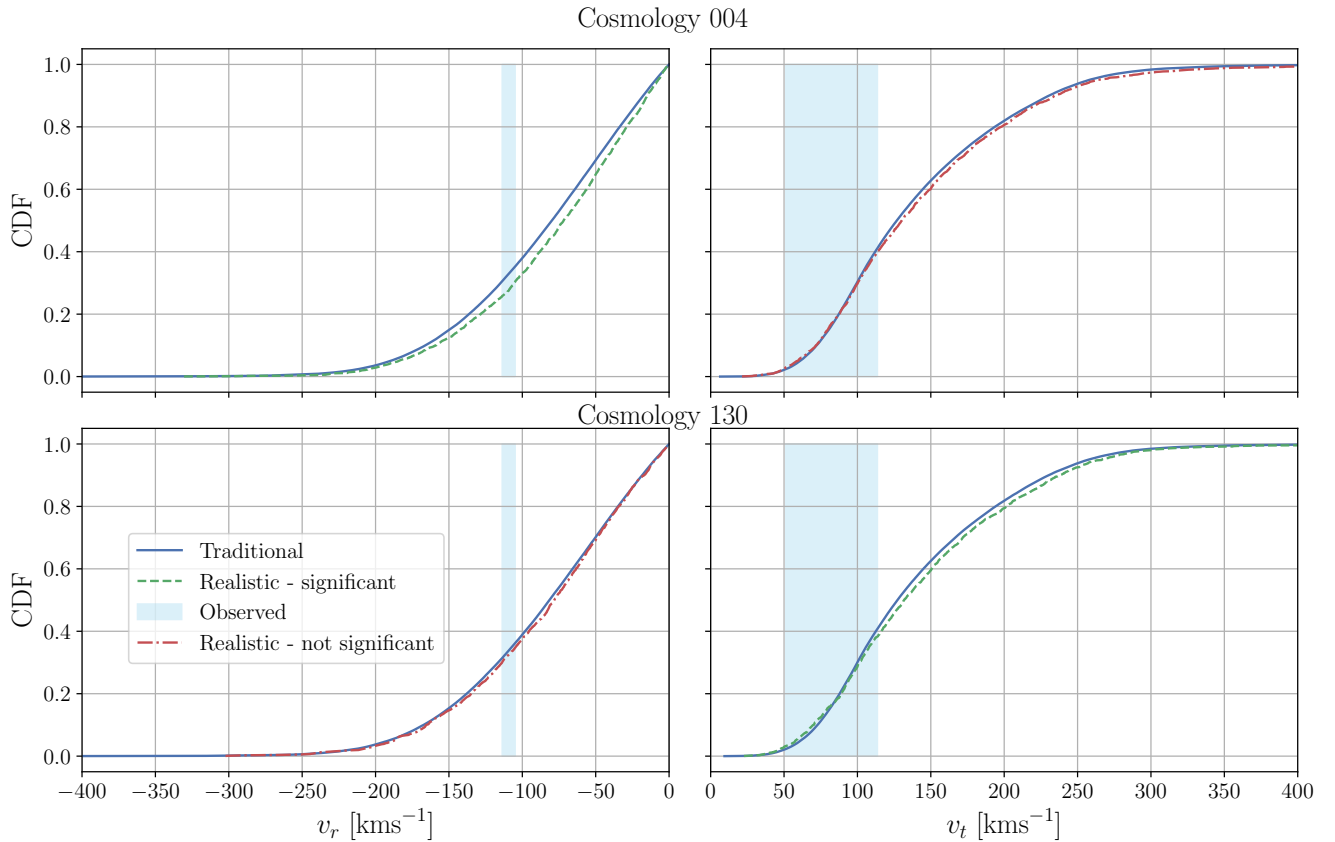


FIG. 5.— Cumulative distributions of M31 velocities relative to the MW. The plots compare observed values with *traditional* and *realistic* LG analogues for the most statistically significant cosmologies. Left panel shows radial velocity (v_r) distributions, and right panel shows tangential velocity (v_t) distributions.

by 5%, indicating a smaller radial speed. The differences in M31's tangential velocity distribution and total mass (M_{LG}) are not statistically significant.

5.2. All cosmologies

Our barycenter velocity constraints consistently affect the distributions of both v_t and v_r compared to traditional constraints across different cosmological models. Figure 3 shows how the mean values of tangential and

radial velocities change across all cosmologies with statistically significant differences according to KS tests. Among the 93 cosmologies we study, the differences in radial velocity distribution are significant in 86 models, while tangential velocity distribution shows significant differences in 11 cosmologies. The effect on total mass (M_{LG}) is also significant in 11 cosmologies. Table 2 summarizes these results.

TABLE 2

AVERAGE OF MEAN VALUES ACROSS COSMOLOGIES FOR DIFFERENT PROPERTIES. ONLY COSMOLOGIES WITH STATISTICALLY SIGNIFICANT DIFFERENCES ARE INCLUDED IN THESE AVERAGES. THE COLUMNS SHOW, RESPECTIVELY: THE PHYSICAL OBSERVABLE, THE SAMPLE TYPE, THE AVERAGE VALUE ACROSS COSMOLOGIES, THE PERCENTAGE DIFFERENCE BETWEEN THE MEAN OF THE SAMPLES, AND THE NUMBER OF COSMOLOGIES (OUT OF 93) WHERE THE DIFFERENCE WAS STATISTICALLY SIGNIFICANT.

Observable	Sample	Mean	Mean difference (%)	Significant cosmologies
$v_r / \text{km s}^{-1}$	Traditional	-85.39	-	86/93
	Realistic	-81.05	-4.86	
$v_t / \text{km s}^{-1}$	Traditional	140.11	-	11/93
	Realistic	141.93	1.42	
$M_{\text{LG}} / 10^{12} M_{\odot}$	Traditional	6.41	-	11/93
	Realistic	6.27	-0.88	

We next investigate which cosmological parameters most strongly determine whether the difference in v_t and v_r between *traditional* and *realistic* pairs is significant. We use a Random Forest algorithm with the KS test p-values as the target variable. We performed a k-fold stratified cross validation and obtained a mean weighted average F1 score of 0.88 for v_r and 0.79 for v_t . It is important to note that due to the class imbalance, the model is skewed towards correctly classifying the majority class, that is, the significant cosmologies in v_r and the not significant in v_t . Figure 6 shows the results, with $\sigma_{8\text{cb}}$ (that is σ_8 taking only into account dark matter and baryons) emerging as the most influential parameter for v_r , and Ω_{cdm} (the dark matter density parameter) for v_t . Figure 7 shows the relationships between the most influential parameters for v_r and v_t . Although we identify this correlation, a deeper exploration of the physical mechanisms explaining why these parameters most strongly affect each velocity component differences remains for future work.

6. CONCLUSION

In this work, we explored the barycenter velocity (\mathbf{v}_b) as a new kinematic constraint for defining Local Group (LG) analogues. This quantity has very low observational uncertainty but was not included in previous studies due to the need for sufficiently large simulation volumes to achieve numerical convergence in peculiar velocities (Forero-Romero & Sierra-Porta 2022). Using simulations from the AbacusSummit project, with a box size of $2 \text{ Gpc } h^{-1}$, we have shown that including this constraint significantly influences the predicted velocity distributions of M31. We demonstrated this effect by comparing LG analogues selected using our proposed constraints (*realistic* pairs) with those selected using traditional constraints (separation distance less than $1 \text{ Mpc } h^{-1}$ and negative radial velocity). Our results show that in the *realistic* pairs, M31 tends to have a smaller radial velocity v_r and larger tangential velocity v_t compared to the *traditional* pairs. We quantified this effect using the difference in means and assessed its significance through two-sample Kolmogorov-Smirnov tests.

This effect is consistent across cosmological models and is particularly robust for v_r . In our analysis of 93 different cosmologies, we found significant differences in the radial velocity distribution for 86 models, while the tangential velocity distribution showed significant differences in 11 cosmologies. The mean differences between *realistic* and *traditional* pairs were 5% for v_r and 1.4% for v_t , averaged across cosmologies.

We also found that $\sigma_{8\text{cb}}$ and Ω_{cdm} are the cosmological

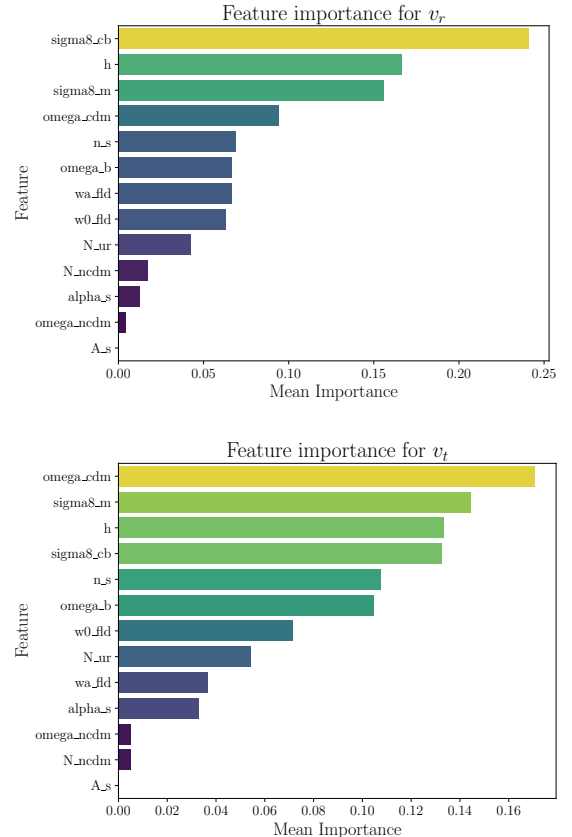


FIG. 6.— Relative importance of various cosmological parameters for predicting whether the difference in M31’s velocities between *traditional* and *realistic* pairs is statistically significant. The top panel shows the parameter importance for v_r , and the bottom panel for v_t . Importance is calculated using a Random Forest algorithm.

parameter that most strongly influences the significance of differences in radial and tangential velocity distributions respectively. However, further work is needed to understand the influence of cosmological parameters on LG kinematics. Similarly, while we have demonstrated statistical differences in velocity distributions, a deeper exploration of the physical mechanisms explaining why barycenter kinematics correlate with orbital properties remains for future work.

In summary, our results show that the kinematic constraints proposed in this work significantly influence the radial and tangential velocities of M31, with effects that are robust across cosmological models. This suggests that these new kinematic constraints should be considered when defining LG analogues in future studies.

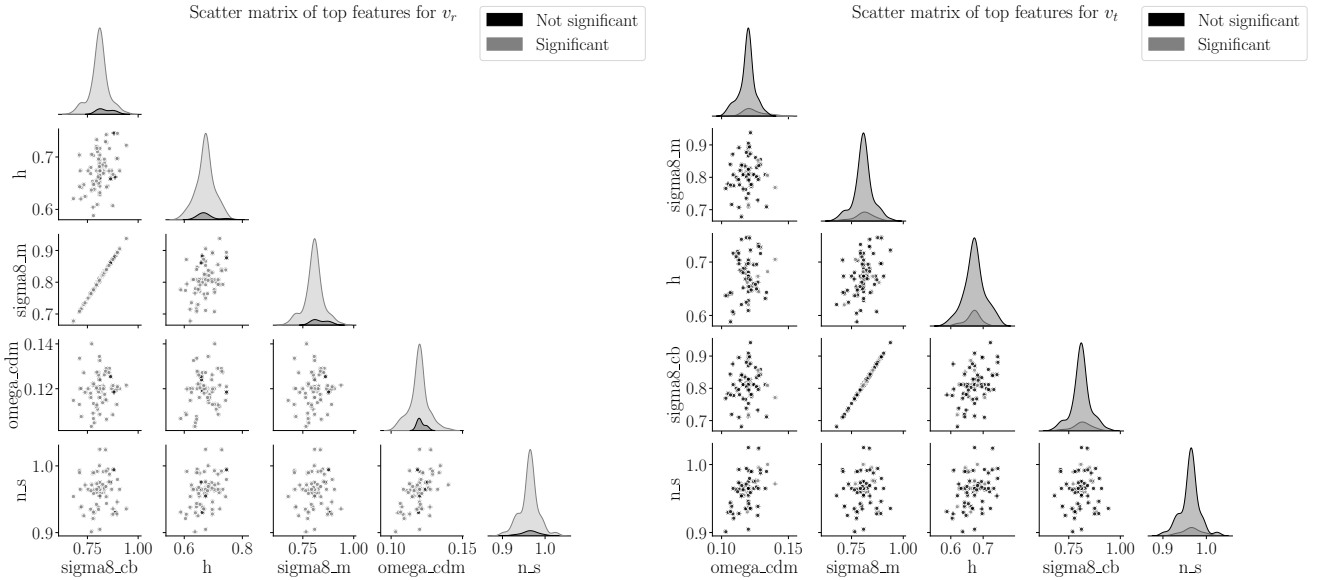


FIG. 7.— Scatter matrix showing pairwise relationships between the most important cosmological parameters for predicting whether a cosmology leads to significant difference in M31’s velocities between *realistic* and *traditional* pairs. The left panel shows the scatter matrix for v_r , and the right panel for v_t .

ACKNOWLEDGMENTS

This work made use of the NASA/IPAC Extragalactic Database (NED), funded by the National Aeronautics

and Space Administration and operated by the California Institute of Technology.

REFERENCES

- Chamberlain, K., Price-Whelan, A. M., Besla, G., et al. 2022, Implications of the Milky Way travel velocity for dynamical mass estimates of the Local Group, arXiv. <http://arxiv.org/abs/2204.07173>
- Evans, I. N., Primini, F. A., Glotfelty, K. J., et al. 2010, The Astrophysical Journal Supplement Series, 189, 37, doi: 10.1088/0067-0049/189/1/37
- Forero-Romero, J. E., Hoffman, Y., Bustamante, S., Gottlöber, S., & Yepes, G. 2013, The Astrophysical Journal, 767, L5, doi: 10.1088/2041-8205/767/1/L5
- Forero-Romero, J. E., & Sierra-Porta, D. 2022, The Astrophysical Journal, 939, 16, doi: 10.3847/1538-4357/ac92ea
- Garrison, L. H., Eisenstein, D. J., Ferrer, D., Maksimova, N. A., & Pinto, P. A. 2021, Monthly Notices of the Royal Astronomical Society, 508, 575, doi: 10.1093/mnras/stab2482
- Hadzhiyska, B., Eisenstein, D., Bose, S., Garrison, L. H., & Maksimova, N. 2021, Monthly Notices of the Royal Astronomical Society, doi: 10.1093/mnras/stab2980
- Hartl, O. V., & Strigari, L. E. 2022, Monthly Notices of the Royal Astronomical Society, 511, 6193, doi: 10.1093/mnras/stac413
- . 2024, The Milky Way and M31 Orbital History: Did the Local Group evolve in isolation?, arXiv, doi: 10.48550/arXiv.2411.07370
- Li, S., Riess, A. G., Busch, M. P., et al. 2021, The Astrophysical Journal, 920, 84, doi: 10.3847/1538-4357/ac1597
- Maksimova, N. A., Garrison, L. H., Eisenstein, D. J., et al. 2021, Monthly Notices of the Royal Astronomical Society, 508, 4017, doi: 10.1093/mnras/stab2484
- McMillan, P. J. 2011, Monthly Notices of the Royal Astronomical Society, 414, 2446, doi: 10.1111/j.1365-2966.2011.18564.x
- Planck Collaboration, Aghanim, N., Akrami, Y., et al. 2020, Astronomy & Astrophysics, 641, A6, doi: 10.1051/0004-6361/201833910
- Salomon, J.-B., Ibata, R., Reylé, C., et al. 2021, Monthly Notices of the Royal Astronomical Society, 507, 2592, doi: 10.1093/mnras/stab2253
- Sawala, T., Teeriaho, M., & Johansson, P. H. 2023, Monthly Notices of the Royal Astronomical Society, 521, 4863, doi: 10.1093/mnras/stad883
- van der Marel, R. P., Fardal, M., Besla, G., et al. 2012, The Astrophysical Journal, 753, 8, doi: 10.1088/0004-637X/753/1/8
- van der Marel, R. P. v. d., Fardal, M. A., Sohn, S. T., et al. 2019, The Astrophysical Journal, 872, 24, doi: 10.3847/1538-4357/ab001b
- Yusef-Zadeh, F., Choate, D., & Cotton, W. 1999, The Astrophysical Journal, 518, L33, doi: 10.1086/312058

This paper was built using the Open Journal of Astrophysics L^AT_EX template. The OJA is a journal which

provides fast and easy peer review for new papers in the **astro-ph** section of the arXiv, making the reviewing process simpler for authors and referees alike. Learn more at <http://astro.theoj.org>.